

# Electroacoustic Properties of Barium Sulfate Particles Coated with a Conductive Layer of Antimony/Tin(IV) Oxides

M. C. Guffond, R. J. Hunter, and J. K. Beattie\*

Heavy Metals Research Centre, School of Chemistry, University of Sydney,  
NSW 2006, Australia

Received January 18, 2001. Revised Manuscript Received May 30, 2001

The dynamic mobility of barium sulfate particles coated with a conducting layer of antimony/tin oxides has been measured with the technique of electroacoustics. Differences between the dynamic mobility spectra of uncoated barium sulfate suspensions and those of the coated particles are observed and attributed to the presence of the conducting surface layer. The magnitude of the complex mobility of the coated particles decreases monotonically with increasing frequency, just as for a nonconducting particle; however, the magnitudes appear to be independent of electrolyte conductivity. The phase angle behavior is also different from that of a low dielectric particle. The change in the phase angle behavior is most obvious at low suspension conductivities and high frequencies where the phase angles show a much smaller phase lag than at higher conductivities. Reasonable agreement between the experimental dynamic mobility spectra and calculated mobilities was found with O'Brien's theory for the enhanced permittivity of semiconductor particles. The results show that electroacoustics could be used to monitor the deposition of these conductive coatings.

## Introduction

Antistatic properties are important in the manufacture, shipment, and use of sensitive electronic parts such as computer chips because these parts need to be protected from electrostatic discharge. Electroconductive coatings are used on the floors, walls, and furniture in the "clean rooms" where electronic parts are produced, and the plastic shipping containers for electronic parts have conductive coatings to prevent electrostatic discharge damage to the parts during shipment. Electroconductive coatings are also used in printing on conductively coated transparent film or paper. Hence, electroconductive powders are used in polymer films, in magnetic recording tapes, on work surfaces, and in paints to impart electroconductive properties.

Antimony-containing tin oxide possesses electroconductivity. We have recently described the electroacoustic behavior of antimony-containing tin oxide colloidal suspensions.<sup>1</sup> These materials, however, impart a blue-black tone due to the doped antimony and have a high production cost. To increase the whiteness of the pigment, the antimony-doped tin oxide can be deposited on titanium dioxide or barium sulfate pigment particles. Such materials have also been found to be electrochromic, with a high contrast ratio.<sup>2,3</sup> A commercial example of coated barium sulfate particles, marketed as Passtran

(or Pastran), is investigated here. We examine the differences between the electroacoustic dynamic mobility spectra of uncoated barium sulfate suspensions and those of the coated particles to determine whether the new technique of electroacoustics can be used to monitor the deposition of conductive coatings and/or to characterize the coated products.

**Electroacoustics.** When an alternating electric field is applied to a suspension of charged particles, they oscillate back and forth. If there is a density difference between the particles and the suspending medium, the oscillation of the particles generates a sound wave known as the electrokinetic sonic amplitude (ESA). The AcoustoSizer (Colloidal Dynamics, Warwick, RI) has been designed to measure the magnitude and phase of the ESA, a complex quantity that depends on the frequency of the applied field. For suspensions of particle volume fraction ( $\phi$ ), it has been shown that the ESA signal can be represented by<sup>4</sup>

$$\text{ESA}(\omega) = A(\omega) \phi \frac{\Delta\rho}{\rho} \langle \mu_d \rangle Z \quad (1)$$

where  $\omega$  is the angular frequency,  $A(\omega)$  is an instrument factor found by calibration,  $\Delta\rho$  is the density difference between the particle and the solvent,  $\rho$  is the density of the solvent,  $Z$  is related to the acoustic impedance of the suspension, and  $\langle \mu_d \rangle$  is the particle-averaged dynamic mobility. The dynamic mobility is a complex quantity and is the high-frequency analogue of the dc electrophoretic mobility. The magnitude of the dynamic

\* To whom correspondence should be addressed. Fax: + 61 2 9351 3329. E-mail: beattiej@chem.usyd.edu.au.

(1) Guffond, M. C.; Hunter, R. J.; O'Brien, R. W.; Beattie, J. K. *J. Colloid Interface Sci.* **2001**, *235*, 371.

(2) Coleman, J. P.; Lynch, A. T.; Puttanachetty, M.; Wagenknecht, J. H. *Sol. Energy Mater. Sol. Cells* **1999**, *56*, 375.

(3) zum Felde, U.; Hasse, M.; Weller, H. *J. Phys. Chem. B* **2000**, *104*, 9388.

(4) O'Brien, R. W.; Cannon, D. W.; Rowlands, W. N. *J. Colloid Interface Sci.* **1995**, *173*, 406.

mobility is the particle velocity per unit field strength. The argument of the dynamic mobility is equal to  $\omega\Delta t$  (radians), where  $\Delta t$  is the time difference between the applied field and the particle velocity. This argument is also referred to as the phase angle of the dynamic mobility; in the case of negative phase angles, it is also called the phase lag. Inertia forces on the particle give rise to a phase lag in the dynamic mobility at high frequencies. This phase lag depends on the particle size and density and on the frequency of the applied field. As a result of the particle inertia effect, it is possible to determine the particle size from electroacoustic measurements.

The dynamic mobility of a spherical particle of radius  $a$  can be written as<sup>1</sup>

$$\mu_d = \frac{\pi \epsilon \zeta \bar{E}}{6 \eta E} G \left( \frac{\omega a^2}{\nu} \right) \quad (2)$$

where  $\epsilon$  and  $\eta$  are the permittivity and viscosity of the solvent, respectively,  $\zeta$  is the zeta potential,  $\bar{E}$  is the average tangential electric field over the particle surface,  $E$  is the applied electric field,  $\nu (= \eta/\rho)$  is the kinematic viscosity, and  $G$  is an inertia factor, given by<sup>4</sup>

$$G(\alpha) = \frac{1 + (1 + i)\sqrt{\frac{\alpha}{2}}}{1 + (1 + i)\sqrt{\frac{\alpha}{2}} + \frac{\alpha}{9}\left(3 + 2\frac{\Delta\rho}{\rho}\right)} \quad (3)$$

where  $\alpha = \omega a^2/\nu$ . This formula can be applied to dielectric, conducting, or semiconducting particles of interest here.

It has been shown that the electric field around a semiconducting particle is the same as that around a dielectric particle with an effective permittivity  $\epsilon_p$  which depends on the ratio of the particle radius to the internal Debye layer thickness  $1/\kappa_1$ .<sup>5</sup> In the typical case when that ratio,  $\kappa_1 a$ , is large,

$$\epsilon_p = \kappa_1 a \quad (4)$$

and the effective permittivity increases with the particle radius.

In our previous work<sup>1</sup> the average tangential field over the particle surface ( $\bar{E}$ ) was shown to have the following form:

$$\bar{E} = \frac{4}{\pi} \frac{3(K + i\omega\epsilon)E}{2K + i\omega(2\epsilon + \epsilon_p)} \quad (5)$$

where  $K$  is the conductivity of the electrolyte. Therefore, at a constant field strength the tangential field around a semiconducting particle depends on the frequency of the applied field and on the electrolyte conductivity of the suspension and is inversely proportional to the particle permittivity. At high frequency there is insufficient time for the ions in the double layer to rearrange themselves to redirect the applied field tangentially to the particle surface, and thus the tangential field is significantly reduced, which causes a minimum in the phase angles. At low frequency, however, there is enough time for the double layer ions to redirect the

applied field tangentially to the particle surface, and the tangential field is comparable to that for a nonconducting particle. As the conductivity of the suspension increases, less time is required for double layer rearrangement, and thus at higher conductivities, there is an increase in the phase lag of the normalized tangential field.

For a nonconducting particle, the tangential field is constant and only the inertia effects of the particle (the  $G$  factor) contribute to the dynamic mobility. The magnitude of the dynamic mobility of a nonconducting particle thus displays a steady decrease with increasing frequency, as does the phase angle, which becomes increasingly negative to the limiting value of  $-45^\circ$ . The dynamic mobility of a semiconducting particle, however, depends not only on particle inertia but also on the variations of the tangential field, the effect of which is to accentuate the decrease in the dynamic mobility magnitude with increasing frequency and to result in a reduced phase lag at high frequency.

## Experimental Section

**Materials and Reagents.** The water used in this study was ultrapure (Milli-Q) water (Millipore, Sydney, Australia) with a conductivity of less than  $1 \times 10^{-6} \Omega^{-1} \text{ cm}^{-1}$  at 20 °C. Sodium nitrate, sodium sulfate, and sodium hydroxide were of analytical grade, were purchased from APS Ajax Finechem, and were used as received. Nitric acid was obtained from BDH and used without further purification.

Passtran (lot no. 981216) was obtained from Mitsui Mining and Smelting Co. Ltd., Tokyo, Japan. The material comprises a barium sulfate core coated with 40 wt % of antimony-doped tin oxide. The resistivity of Passtran was stated by the manufacturer to be 30  $\Omega$  cm, with a specific density of 4.8 g/cm<sup>3</sup>, a median size of 0.4  $\mu\text{m}$ , and a size distribution of 0.12–1.61  $\mu\text{m}$ . Barium sulfate (Hombitan HX, lot no. 040057014) was obtained from Sachtleben Chemie GmbH, Duisburg, Germany. The manufacturer's information stated that the average particle size was approximately 0.6  $\mu\text{m}$  and that the surface was uncoated. Both powders were used without further purification.

**Preparation of Suspensions.** A 2% particle volume fraction suspension of Passtran was prepared by adding water (370 g) to Passtran (35.52 g) in a 500 mL polyethylene bottle. The suspension was then dispersed by ultrasonication at its natural pH (2.4) for 5 min with a Branson 450 sonifier with a 1.9 cm diameter horn. The frequency of operation was 20 kHz, and the power output was maintained at 50% of the limiting power (350 W). The suspension was then left overnight. The natural conductivity of this suspension of Passtran was 0.07 S/m.

A 2% particle volume fraction of BaSO<sub>4</sub> was prepared by adding water (370 g) to barium sulfate (33.3 g) in a 500 mL polyethylene bottle. The resulting suspension was then sonicated for 30 min in a sonic bath (Branson 5210). The suspension was then left overnight on an orbital mixer (Retek Instruments, Boronia, Australia).

**Electroacoustic Measurements.** To increase the signal-to-noise ratio, the ESA signal of the Passtran suspension was averaged over 1024 measurements at each frequency, instead of over the standard 36 measurements, and the ESA signal of barium sulfate was averaged over 1600 measurements at each frequency. This ensured that the measured signal was free from any significant noise and increased the measurement time from 3 to 10 min for Passtran and to 17 min for barium sulfate.

Once the Passtran suspension was in the AcoustoSizer cell, the pH was adjusted to and then maintained at 3.6 by the dropwise addition of NaOH (1 M) or HNO<sub>3</sub> (1 M). The first measurement was taken without the addition of any additional electrolyte. The conductivity of the suspension was increased

for subsequent measurements by the dropwise addition of a concentrated  $\text{NaNO}_3$  solution. This was done in the AcoustoSizer cell while the suspension was being stirred.

The surface of barium sulfate has very little charge, and hence it was charged with the addition of a potential determining ion by the dropwise addition of a concentrated  $\text{Na}_2\text{SO}_4$  solution until conductivity of the suspension was comparable to that of the Passtran suspension at its lowest conductivity. The pH was maintained at  $3.65 \pm 0.02$ , and the conductivity of the suspension was increased for subsequent measurements in the manner described above for Passtran.

Background measurements were made for each of the colloid measurements. This was done by the dropwise addition of a saturated solution of the appropriate salt until a conductivity comparable to that of the corresponding colloid measurement was reached. Small amounts of very dilute  $\text{NaOH}$  and  $\text{HNO}_3$  solutions were used to adjust the pH of the background solution to that of the colloid measurements.

**Electrophoresis Measurements.** The dc electrophoretic mobility of Passtran was determined with a Delsa 440 (Coulter Electronics). Dilute suspensions of Passtran [0.01% (w/v)] were prepared by the dilution of a stock suspension of 0.1% (w/v). The pH and conductivity of the resulting suspension were adjusted to values comparable to those used in the electroacoustic measurements. This was accomplished with the dropwise addition of dilute  $\text{HNO}_3$  or  $\text{NaOH}$  solutions and of a concentrated  $\text{NaNO}_3$  solution. The electrophoretic  $\zeta$  potential was then determined using the theory of O'Brien and White.<sup>6</sup>

## Results

**Electroacoustic Results.** The dynamic mobility spectra of barium sulfate at three different suspension conductivities are shown in Figure 1 (symbols), along with the theoretical mobilities (lines) calculated with the standard electroacoustic theory with an input value of 11.4 for the particle permittivity.<sup>7</sup> The parameters obtained from the theoretical fits to the experimental data are given in Table 1. The magnitudes of the dynamic mobility of barium sulfate are negative as a result of the addition of the potential determining sulfate ion to the suspension. The magnitudes are on the order of  $10^{-9} \text{ m}^2 \text{ V}^{-1} \text{ s}^{-1}$ , which is relatively small. The magnitude of the ESA signal could have been increased by the addition of more  $\text{Na}_2\text{SO}_4$  to increase the negative surface charge on the barium sulfate particles. This was not done, however, so that the conductivity of the suspension would be similar to that of the following Passtran sample. The median size of  $0.62\text{--}0.67 \mu\text{m}$  as determined by the standard theory used in the AcoustoSizer software agrees well with the manufacturer's specification of a median size of approximately  $0.6 \mu\text{m}$ . The agreement between the theoretical and experimental magnitudes is excellent. The magnitudes decrease monotonically with increasing frequency (as the particles lag further behind the applied field), and they also decrease with increasing suspension conductivity, reflecting the usual compression of the double layer with increasing ionic strength.

The phase angles decrease regularly with increasing frequency and are independent of the conductivity of the suspension. The high-frequency phase angles of barium sulfate exceed  $45^\circ$ , which is the theoretical maximum for a dielectric particle with a thin double

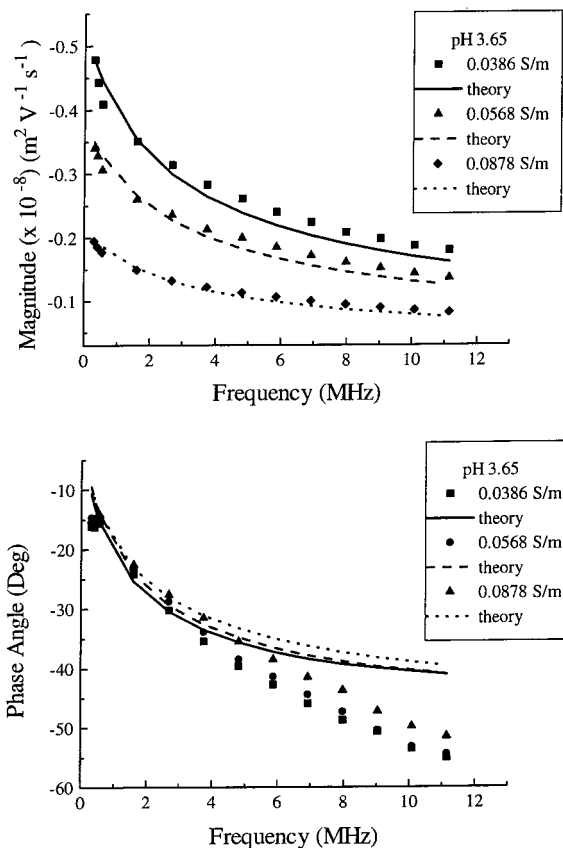


**Figure 1.** Comparison of the theoretical (lines) to experimental (symbols) dynamic mobility spectra of barium sulfate (2%) with increasing electrolyte conductivity ( $\text{NaNO}_3$ ), pH 3.65.

**Table 1. Size and  $\zeta$  Potential for  $\text{BaSO}_4$  at Three Suspension Conductivities (pH 3.65) As Determined from the Dynamic Mobility Spectra of Figure 1**

conductivity (S/m)	median diameter ( $\mu\text{m}$ )	68% size range ( $\mu\text{m}$ )	$\zeta$ potential (mV)	fit error (%)
0.0386	0.63	0.25–1.54	-7.5	11.2
0.0568	0.62	0.27–1.43	-5.4	11.0
0.0878	0.67	0.28–1.57	-3.1	9.6

layer (Figure 1). At high frequencies the difference between the experimental and theoretical phase angles is as much as  $15^\circ$ . This could be a result of particles sticking to the electrodes because of their low surface charge. The anomalous phase angles account for the high fit error, which is the relative root-mean-square error between the calculated and observed dynamic mobilities. At low frequencies the agreement between theory and experiment is good.

Figure 2 displays the dynamic mobility spectra of Passtran at pH 3.64 at various suspension conductivities. The magnitudes are reasonably large (on the order of  $2 \times 10^{-8}\text{--}7 \times 10^{-9} \text{ m}^2 \text{ V}^{-1} \text{ s}^{-1}$ ) and decrease regularly with increasing frequency. They are also nearly independent of the conductivity of the suspension. The phase angles display a strong dependence on the conductivity of the suspension. At lower electrolyte conductivities, there is a significant reduction of the phase lag at higher frequencies, resulting in a minimum in the phase angles. At the higher conductivity measurements, however, the phase angles behave in a manner typical of a dielectric particle, becoming monotonically more negative with increasing frequency.

(6) O'Brien, R. W.; White, L. R. *J. Chem. Soc., Faraday Trans. II* **1978**, *74*, 1607.

(7) Young, K. F.; Frederikse, H. P. R. *J. Phys. Chem. Ref. Data* **1973**, *2*.

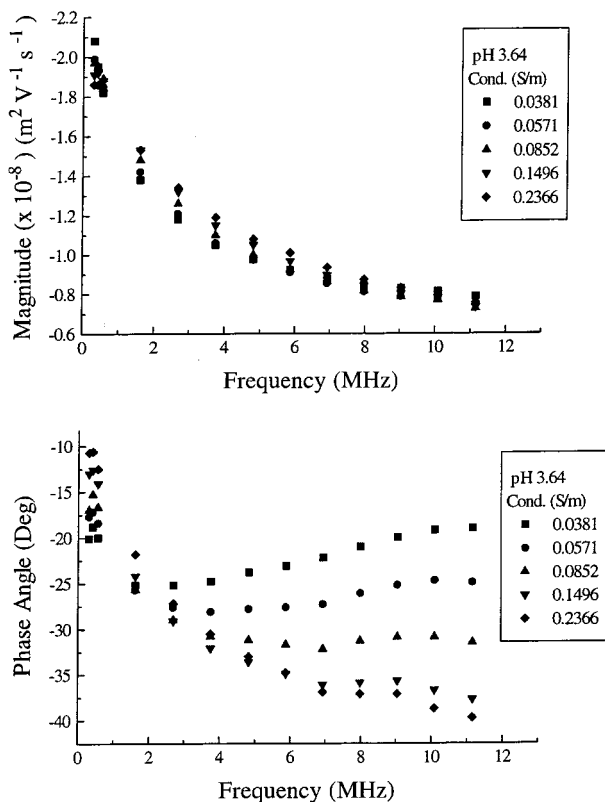


**Figure 2.** Dynamic mobility spectra of Passtran (2%) as a function of frequency with increasing electrolyte conductivity ( $\text{NaNO}_3$ , pH 3.64).

**Table 2. Apparent Size and Charge Data for Passtran at Various Suspension Conductivities (pH 3.64) As Calculated for a Dielectric Particle with  $\epsilon_p$  of 100 from the Dynamic Mobility Spectra of Figure 2**

conductivity (S/m)	median diameter ( $\mu\text{m}$ )	68% size range ( $\mu\text{m}$ )	$\zeta$ potential (mV)	fit error (%)
0.0381	9.96	0.28–353.84	–129.0	2.1
0.0571	10.40	0.42–260.38	–108.1	3.6
0.0852	3.09	0.37–25.68	–62.8	5.5
0.1496	0.72	0.32–1.60	–31.8	4.3
0.2366	0.58	0.34–0.98	–28.1	2.5

The dynamic mobility spectrum measured at the highest conductivity was successfully fitted to the theory for a dielectric particle with a particle permittivity,  $\epsilon_p$ , of 10, typical for a nonconducting oxide. The  $\zeta$  potential was calculated to be  $-27$  mV, with a median diameter of  $0.57 \mu\text{m}$  and a spread from  $0.42$  to  $0.79 \mu\text{m}$ , with a fit error of 2.8%. However, dynamic mobilities at the lower electrolyte conductivities display reductions in phase lags at higher frequencies that are inconsistent with this simple model. With a larger particle permittivity of 100 (similar to that of rutile), the  $\zeta$  potential and size could be calculated from the measured dynamic mobility at each conductivity of the suspension with a reasonable fit error (Table 2). To do so, however, the software algorithm was sometimes forced into quite unrealistic values for the unknowns. To account for the reduction in phase lag at high frequency, the  $\zeta$  potential was increased to very high values (to introduce significant double layer distortion); then, to compensate for the apparently low magnitudes, the particle size was simultaneously increased to values well outside the instrument measuring range. These effects are more marked at low electrolyte conductivities, which leads

to a very strong dependence of the “apparent” properties on the suspension conductivity (Table 2). This is most unusual and is a very good indication that there is something unusual about the dynamic mobility of these particles.

At the highest suspension conductivity, the  $\zeta$  potential, median diameter, and size range calculated with  $\epsilon_p$  of 100 are nearly identical with those calculated with  $\epsilon_p$  of 10. This confirms that, at the highest electrolyte conductivity, the dynamic mobility is similar to that which would be expected for a nonconducting particle, because the determination of size and charge of a dielectric particle is not very sensitive to the value of  $\epsilon_p$ .

To fit the experimental dynamic mobility spectra with more realistic values for the  $\zeta$  potential and particle size, the enhanced particle permittivity was set to the limiting value of  $\kappa_1 a$ , where  $\kappa_1$  is the thickness of the internal double layer of a semiconductor due to the internal charge carriers and  $a$  is the particle radius (eq 4). This model was derived for semiconducting particles which consist of 100% semiconducting material, but it has been shown that it is also applicable to semiconductors with a conductive shell around a dielectric core.<sup>9</sup> The enhanced permittivity for a chosen value of  $\kappa_1$  was calculated for the size range of  $0.1$ – $10 \mu\text{m}$  with a Microsoft Excel spreadsheet program. Within the program, median and minimum diameters are specified from which the maximum diameter is calculated based on a log-normal distribution.

The  $\zeta$  potential is the additional parameter required to calculate the dynamic mobility. The standard theory used in the AcoustoSizer software yielded a value of  $-28.1$  mV at the highest conductivity, which agreed with the estimated value from the dc electrophoresis at the lowest conductivity of  $-28.6$  mV, described below. Two choices were therefore considered: maintain the  $\zeta$  value at  $-28.6$  mV for all conductivities or reduce it gradually with increasing conductivity in accordance with the usually observed behavior of double layer compression. There is little to choose between the two approaches. We have elected to reduce it in steps of 1 mV for a total of 5 mV from the lowest to highest conductivity, as the physically more realistic model.

The median diameter was chosen to be  $0.4 \mu\text{m}$  because this is the value stated by the manufacturers. Initially the minimum diameter was chosen to be  $0.12 \mu\text{m}$  as also stated by the manufacturers, which left just the internal double layer thickness ( $\kappa_1$ ) as the only adjustable parameter. It was found that it was not possible to obtain acceptable fits of the experimental data by adjusting  $\kappa_1$  alone. Hence, the minimum diameter also was used as an adjustable parameter. Altering the minimum diameter (while maintaining a constant median diameter) merely affects the size distribution, making the sample appear either more polydisperse or more monodisperse. To obtain reasonable fits over the whole conductivity range, the above two parameters were manually adjusted by trial and error until an acceptable visual fit for the lowest conductivity mea-

(8) Carasso, M. L. *The Effect of Polymer Adsorption on the Electroacoustic Signals of Colloidal Silica*; University of Sydney: Sydney, Australia, 1996; p 36.

(9) O'Brien, R. W. Personal communication, 1999.

surement was obtained. These chosen values for the minimum diameter and the internal double layer were then used to fit the highest conductivity measurement, with a corresponding decrease in  $|\zeta|$  of 5 mV. However, to produce an acceptable fit for the highest conductivity measurement, further refinement of the values found for the lowest conductivity measurement was required. Using the refined values, the lowest conductivity measurement was then used to further readjust the parameters. This process was repeated several times until values for the minimum diameter and  $\kappa_1$  gave reasonable fits at both the highest and lowest conductivity measurements. This method of fitting the data also resulted in reasonable fits at the middle conductivity measurements. The final value selected for  $\kappa_1$  was  $1200 \mu\text{m}^{-1}$ . This implies that the thickness of the internal double layer due to the charge carriers is on the order of 1 nm. This is similar to the value of  $\sim 1500 \mu\text{m}^{-1}$  found by Hunter and O'Brien for phosphorus-doped silicon.<sup>10</sup> The final value selected for the minimum diameter was  $0.1 \mu\text{m}$  and, hence, the maximum diameter was calculated to be  $1.60 \mu\text{m}$ . Thus, once a size distribution and a value for  $\kappa_1$  were found, these parameters remained fixed and only the  $\zeta$  potential was decreased (slightly) as the conductivity of the suspension increased. Hence, the same set of parameters was used to fit the dynamic mobility spectra at the five different conductivities. Parts a–e of Figure 3 show the theoretical fits, on the same scale, of the experimental dynamic mobility spectra.

**Electrophoresis.** The dc electrophoretic mobility of Passtran at pH 3.66 and a suspension conductivity of  $0.0413 \text{ S/m}$  was determined to be  $-2.0 \pm 0.1 \times 10^{-8} \text{ m}^2 \text{ V}^{-1} \text{ s}^{-1}$ . This is identical (within experimental error) with the magnitude at 0.3 MHz (corrected for particle inertia) of  $-2.1 \times 10^{-8} \text{ m}^2 \text{ V}^{-1} \text{ s}^{-1}$  at pH 3.67 and a suspension conductivity of  $0.0381 \text{ S/m}$ .

### Discussion

The magnitudes of the dynamic mobility of barium sulfate show a strong dependence on the conductivity of the suspension, decreasing with increasing electrolyte conductivity. This is a reflection of the usual compression of the double layer and hence the reduction in the absolute  $\zeta$  potential ( $|\zeta|$ ) with increasing ionic strength. This indicates that the barium sulfate behaves as a dielectric particle, as expected. There is good agreement between experimental and theoretical magnitudes of the dynamic mobility spectra calculated with the polarizable thin double layer theory for dielectric particles.

The phase angles of barium sulfate are independent of the conductivity of the suspension, and the phase lag increases in a monotonic fashion with increasing frequency, which suggests that only inertial forces (the  $G$  factor of eq 3) contribute to the phase lag. The experimental phase angles at low frequencies agree well with those generated by the theory. At higher frequencies, however, the experimental phase angles are as much as  $15^\circ$  larger than the theoretical limiting of  $45^\circ$ . The low magnitudes for  $\text{BaSO}_4$  are indicative of low surface charge and hence of the instability of the system. Thus, the particles are probably not well dispersed, and there

may be particles adhering to the electrodes. The effect of this is to increase the distance the ESA signal has to travel down the delay rod, and this increases the measured phase lag. If the particle size is much less than the wavelength of the ESA signal, particles sticking to the electrodes have no significant effect. However, over the high-frequency range of the AcoustoSizer, particles of approximately  $1 \mu\text{m}$  in size can increase the phase lag by several degrees,<sup>8</sup> thus making the phase lag surpass the theoretical maximum of  $45^\circ$ . Because of the low surface charge of the particles in this system and their apparent size of  $\sim 0.6 \mu\text{m}$ , it would be more likely that aggregates and not individual particles adhering to the electrodes would give rise to this effect.

The magnitudes of the dynamic mobility of the Passtran suspensions are largely unaffected by the increasing conductivity of the suspension. The theory for a semiconducting particle, however, predicts that at a fixed frequency the magnitude of the tangential field (and hence the magnitudes of the dynamic mobility) should decrease with decreasing electrolyte conductivity. This discrepancy between theory and experiment may be due to the relatively high resistivity of Passtran ( $30 \Omega \text{ cm}$ ). That is, the conductive effects of the particles are not sufficiently large to affect the magnitudes in the manner predicted by the theory. Based on the manufacturer's specifications of a median diameter of  $0.4 \mu\text{m}$  with 40 wt % of the sample consisting of antimony-doped tin oxide, the conductive layer of the particles was calculated to be approximately 23 nm, approximately 10% of the particle radius. Therefore, the conductive layer around these particles is reasonably thin. The good agreement between the dc electrophoretic mobility and the magnitude of the dynamic mobility at 0.3 MHz (corrected for particle inertia) also implies that the magnitudes are unaffected by the conductive layer of the particles.

Comparison of the phase angle curves of Passtran to those of barium sulfate indicates that the Passtran suspensions do not behave as dielectric particles, because the phase lag of the dynamic mobility of Passtran varies with the suspension conductivity. The strong dependence of the phase angles on the conductivity of the suspension is most likely due to the conducting layer of the particles and the charge rearrangement in the diffuse part of the double layer. The buildup and depletion of diffuse double layer charge around each half of a semiconducting particle during one cycle of the field cause a phase lag in the tangential field. The time required for this rearrangement of ions decreases with increasing electrolyte conductivity. Thus, for lower conductivity measurements of Passtran in the high-frequency range of the AcoustoSizer, there is not enough time for this charge rearrangement to occur, and hence there is a significant reduction in the phase lag of the tangential field. This translates to a reduction in the phase lag of the dynamic mobility at high frequency. These changes in the phase lag of the dynamic mobility with electrolyte conductivity are in agreement with the theoretical model presented in the Introduction.

At the lowest conductivity (Figure 3a), the theoretical magnitudes underestimate the experimental magnitudes by about 15%. Increasing the  $\zeta$  potential to  $-35 \text{ mV}$  would give excellent agreement between the ex-

(10) Hunter, R. J.; O'Brien, R. W. *Colloids Surf. A* **1997**, *126*, 123.

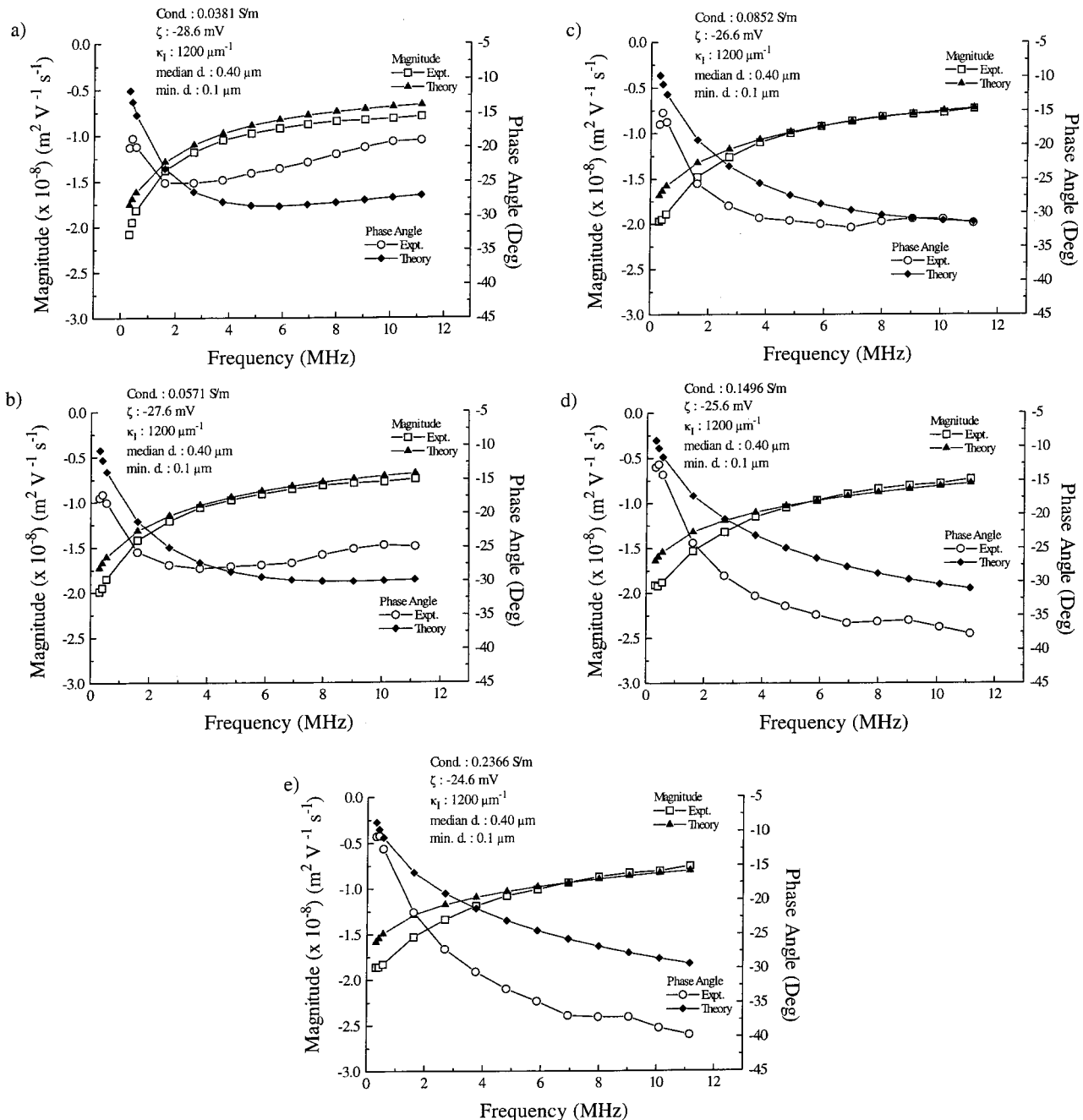


**Figure 3.** Comparison of theoretical fits (solid symbols) to the experimental (open symbols) dynamic mobility of Passtran (2%) at pH 3.64 (median diameter  $0.4 \mu\text{m}$ , minimum diameter  $0.1 \mu\text{m}$ , semiconductor factor ( $\kappa_1$ )  $1200 \mu\text{m}^{-1}$ ): (a)  $\zeta$  potential  $-28.6 \text{ mV}$ ,  $0.0381 \text{ S/m}$ ; (b)  $-27.6 \text{ mV}$ ,  $0.0571 \text{ S/m}$ ; (c)  $-26.6 \text{ mV}$ ,  $0.0852 \text{ S/m}$ ; (d)  $-25.6 \text{ mV}$ ,  $0.1496 \text{ S/m}$ ; (e)  $-24.6 \text{ mV}$ ,  $0.2366 \text{ S/m}$ .

perimental and theoretical magnitudes. The theoretical phase angles capture the general shape of the experimental ones, with an initial phase lag that decreases with increasing frequency. Nevertheless, the theory overestimates the degree of phase lag.

As the electrolyte conductivity increases and the  $\zeta$  potential decreases, the agreement between theoretical and experimental magnitudes improves at the higher frequencies but declines somewhat at the lower frequencies. This is because at high frequency the theoretical magnitudes increase with conductivity (in accord with theory), yet at low frequency they decrease slightly with increasing conductivity because of the decrease in the  $\zeta$  potential, while the experimental magnitudes are independent of the electrolyte conductivity. This could

be overcome by maintaining a constant  $\zeta$  potential, but this results in the theoretical magnitudes overestimating the high-frequency experimental ones. Maintaining a constant  $\zeta$  potential makes no difference to the phase angles.

Over the whole conductivity range, the theoretical phase angles capture the overall shape and trends of the experimental ones. As the conductivity of the suspension increases, the minimum in the phase lag in the tangential field occurs at higher frequencies (as reflected in the phase angles), in accordance with theory. However, the theoretical phase angles at the lowest conductivities overestimate the phase lag and underestimate it at the higher conductivities. This was also found for another system in a previous study,<sup>1</sup> implying

that another parameter needs to be added to the theory.

It was found that increasing or decreasing  $\kappa_1$  by no more than  $200 \mu\text{m}^{-1}$  from the chosen value of  $1200 \mu\text{m}^{-1}$  with the other parameters held constant made little difference to the theoretical fits. Increasing  $\kappa_1$  by more than  $200 \mu\text{m}^{-1}$  resulted in theoretical magnitudes significantly lower than the experimental ones at low conductivity. The theoretical phase angles significantly underestimated the phase lag at high conductivity when  $\kappa_1$  was decreased by more than  $200 \mu\text{m}^{-1}$ .

The qualitative agreement shown in Figure 3 between the experimental and theoretical dynamic mobility spectra has been achieved by incorporating the semiconductor factor into the dynamic mobility equations. This leads to a set of parameters that accurately reflect the physical aspects of the system based on the median size supplied by the manufacturers and the  $\zeta$  potential obtained from electrophoresis measurements. In contrast, in the absence of the semiconductor factor, the theory for a dielectric particle gave physically unrealistic results except at the higher electrolyte conductivities (Table 2). This demonstrates that a naive application

of the simple electroacoustic theory can give satisfactory fits to the experimental data but misleading results. In the present case the conductivity dependence of the phase angles reveals the conducting nature of the surface coating.

The conducting layer is typically deposited on the nonconducting dielectric core particle under conditions of high electrolyte concentration. In these circumstances the  $\zeta$  potential calculated from the simple theory for a dielectric particle could be used to monitor the deposition of the surface coating. Resuspension of the coated particles in a solution of low conductivity would then reveal the anomalous phase angle spectrum associated with the conducting layer.

**Acknowledgment.** We thank Drs. Richard O'Brien and William Rowlands of Colloidal Dynamics Pty. Ltd., Sydney, Australia, for helpful discussions and technical assistance.

CM010045E